Lasers in Surgery and Medicine 23:263–273 (1998)

Photodynamic Therapy With Local Photosensitizer Delivery Inhibits Experimental Intimal Hyperplasia

Farzin Adili, MD,[1,3] Randolph G. Statius van Eps, MD,[1,3] Thomas J. Flotte, MD,[2,3] and Glenn M. LaMuraglia, MD[1,3]*

[1] Division of Vascular Surgery, Massachusetts General Hospital and Harvard Medical School, Boston, Massachusetts 02114
[2]Department of Pathology, Massachusetts General Hospital and Harvard Medical School, Boston, Massachusetts 02114
[3]Wellman Laboratories of Photomedicine, Massachusetts General Hospital and Harvard Medical School, Boston, Massachusetts 02114

Background: **Photodynamic therapy (PDT), the light activation of photosensitizer dyes for the production of free radicals, effectively inhibits experimental intimal hyperplasia with systemic administration of the photosensitizer. The local application of the photosensitizer directly into a vascular lesion to avoid systemic side effects and tightly control dose administration has theoretical appeal. The aim of this study was to quantify serum and arterial tissue uptake after site-specific photosensitizer delivery and, following PDT, determine its effectiveness at inhibiting intimal hyperplasia.**
Study Design/Materials and Methods: **The rat common carotid artery was balloon-injured, pressurized at 400 mm Hg for 2 minutes with the photosensitizer dye benzoporphyrin-derivative (BPD), and irradiated with 690 nm laser light at a fluence of 100 J/cm^2. Control animals were pressurized with saline only, or received no additional treatment than balloon-injury.**
Results: **Pressurization with BPD resulted in complete penetration of the intima and media and was associated with relatively high tissue, but almost no detectable serum BPD concentrations. No skin photosensitization or other systemic side effects were observed with photosensitizer administration. After 9 days, PDT-treated arteries displayed a significantly lower number of smooth muscle cells in the arterial wall than balloon-injured ($P < 0.001$) or saline-pressurized arteries ($P < 0.0002$), and no intimal hyperplasia. At 21 days, IH after PDT was significantly reduced as compared with balloon-injured ($P < 0.0004$), or saline-pressurized arteries ($P < 0.003$) with no arterial dilatation.**
Conclusions: **Site-specific delivery of liposomal BPD followed by**

Contract grant sponsor: NIH; Contract grant number: HL 02583; Contract grant sponsor: Office of Naval Research; Contract grant number: N00014-91-C-0084; Contract grant sponsor: Deutsche Forschungsgemeinschaft; Contract grant number: Ad 106/2-1 (to F.A.); Contract grant sponsor: Dutch Heart Association; Contract grant number: R94138.

*Correspondence to: Glenn M. LaMuraglia, M.D., Massachusetts General Hospital, ACC 464 Boston, MA 02114.

Accepted 4 August 1998

PDT represents a safe method to treat arteries, and may be effectively used *in vivo* to inhibit the development of intimal hyperplasia. Lasers Surg. Med. 23:263–273, 1998.

INTRODUCTION

Early restenosis after invasive vascular interventions remains the major limitation to a satisfactory long-term result [1]. A key mechanism that has been implicated with the development of early luminal renarrowing is intimal hyperplasia (IH), the unrestrained proliferative and migratory response of smooth muscle cells at the site of vascular injury. This process is associated with increased synthesis and deposition of extracellular matrix in the subendothelium that leads to loss of area in the lumen.

To date, a variety of different therapeutic modalities mechanically to remove or overcome obstructing vascular lesions, such as balloon angioplasty, intraluminal stents, atherectomy, and endarterectomy, have been developed and advocated [2]. Additionally, numerous drugs[3] and gene therapy [4,5] have been studied in laboratory experiments. By reducing proliferation and migration of smooth muscle cells, favorable effect was expected on the development of IH in the clinical setting. Unfortunately, the success of these techniques has thus far been limited.

Photodynamic therapy (PDT) is an effective, alternate experimental approach to prevent IH. It precisely eradicates cells from targeted segments of the vascular wall without causing inflammation, structural deterioration of the blood vessel wall, or vascular occlusion [6,7]. PDT represents an application of phototherapy in which wavelength-specific light is applied to activate otherwise relatively nontoxic photosensitizer dyes (photosensitizer). Following the absorption of photons, the photosensitizer is transformed into an excited state from where it can either directly form free radicals, or transfer its energy to molecular oxygen to produce singlet oxygen. These moieties are thought to exert cytotoxic effects by lipid peroxidation and protein denaturation of cellular membranes and organelles [8,9]. Since the half-life of the free-radicals are short-lived, ranging from nano- to microseconds, the cytotoxic effects are strictly limited to the area where the photosensitizer is activated. PDT targeting to the injured area in the arterial wall is possible after systemic photosensitizer delivery because of directed light-irradiation and selectivity is enhanced by the characteristic partitioning of the photosensitizer in proliferating cells [10].

Despite confined light irradiation, the site-specific delivery of photosensitizer directly into a vascular lesion has theoretical appeal [11]. First, it would achieve concentration-controlled, local drug concentrations in a relatively short period of time, even if the agent is rapidly cleared or metabolized. Second, by concentrating the drug at the target site and thus avoiding substantial systemic dosing, systemic adverse effects such as photosensitization of the skin could be minimized and a prolonged effective concentration of the drug in the target lesion may be attained. Third, by utilizing specific local, luminal delivery parameters, ideally there would be no photosensitizer in the perivascular tissues and any scattered light administered with PDT would not result in injury to adjacent veins, nerves, or other tissues.

The drug Benzoporphyrin-derivative monoacidic ring A (BPD) belongs to the class of second-generation photosensitizers. These new molecules are proposed as possible alternatives to the porphyrin mixtures, hematoporphyrin derivative, and Photofrin®, the only photosensitizers that to date have been extensively tested in clinical trials with PDT [12–14]. Unlike the first-generation photosensitizer, BPD's skin photosensitivity rapidly disappears after administration. It has a high light absorption at 690 nm, a wavelength of visible light well suited to tissue penetration [13]. BPD, as most photosensitizers, produces singlet oxygen, which is thought to be the most important free-radical responsible for the cytotoxic effects. In intact blood vessels, an important mechanism of vascular targeting by these photosensitizers has been the binding to endogenous low density lipoproteins (LDL) in proliferating cells and in the serum providing receptor-mediated binding to endothelial cells via the regular LDL pathway [14,15]. Benzoporphyrin-derivative was used as BPD-monoacid ring A prepared in the formulation of unilamellar liposomes. Intravascular redistribution of BPD from liposomes to LDL with subsequent membrane binding has been shown to be a characteristic feature of liposomal BPD-uptake [15].

Therefore, this study was designed to deter-

mine how effective local photosensitizer delivery is for PDT in vascular applications. The uptake and distribution of locally delivered photosensitizer will be determined. Using this approach for PDT, the inhibition of IH will be assessed in the rat carotid balloon injury model.

MATERIALS AND METHODS

Experimental Design

Male Sprague Dawley rats (Charles River Breeding Laboratories, Wilmington, MA), weighing 350–450 g, were anesthetized with intramuscular Ketamine (75 mg/kg), Xylazine (5 mg/kg), and Atropine (40 μg/kg). A midline neck incision was performed and the left carotid artery exposed. After clamping the common carotid artery and the internal carotid artery with Heifitz clamps, a 2 F Fogarty embolectomy catheter (Baxter Health Care, Irvine, CA) was introduced into the external carotid artery. The common carotid artery was subsequently mechanically injured by inflating the balloon with 0.2 ml air and gently passing and rotating the catheter three times within the clamped area of the distal common carotid artery.

The animals were randomly assigned to following three groups: group "PDT" received photosensitizer by local delivery of the drug to the left common carotid artery. Animals in group "PR" (saline-pressurization only) had the left carotid artery pressurized with saline only. Group "BI" (balloon-injury) did not receive any treatment other than balloon-injury to the carotid artery.

Local Delivery

After balloon-injury, a 22 G polyethylene catheter was advanced through the external carotid artery into the distal portion of the common carotid artery and secured with a suture. The tube was connected via three-way stopcock to a Statham transducer for synchronous pressure monitoring with a digital pressure manometer (HP 78205C, Hewlett Packard, Corvallis, OR). Benzoporphyrin-derivative (BPD-MA verteporfin®, Quadra Logic Technologies, Vancouver, BC, Canada), provided as a liposomal preparation, was reconstituted in distilled water (2 mg/ml) and diluted in physiologic saline to a final concentration of 25 μg/ml. Under low ambient light, the drug was injected into the clamped artery with a pressure of 400 mm Hg for 2 minutes. Following the aspiration of BPD from the arterial lumen, the artery was flushed with saline, the catheter was removed, blood flow was restored to the internal carotid artery, and the external carotid artery was ligated.

Photodynamic Therapy

Fifteen minutes after local delivery, the common carotid artery was externally irradiated with 690 nm laser light, emitted by an argon-pumped dye laser (Coherent Innova I 100 and Coherent CR 599, Coherent, Palo Alto, CA) to deliver a total fluence of 100 J/cm^2 at an irradiance of 100 mW/cm^2. The dye laser was coupled to a 600-μm optical fiber, and a 5-mm focal length lens was used to magnify the output end of the optical fiber to obtain a uniform 2-cm spot. The targeted artery was submerged in physiologic saline, placed on a right-angled reflective mirror, and optically isolated with black, light-impervious tape to avoid irradiation of surrounding tissue. At the conclusion of the irradiation, the mirror was removed and the wounds closed by standard surgical technique. All procedures were approved by an independent institutional animal care committee. Animal care complied with the "Principles of Laboratory Animal Care" and the "Guide for the Care and Use of Laboratory Animals" (NIH Publication No. 80-23, revised 1985).

Harvest

The rats were sacrificed after 9 (n = 9), and 21 days (n = 11) for microscopic analysis, which included morphometric analysis and immunohistochemistry. Following cannulation of the iliac artery, the arterial system was flushed with saline, and in situ perfusion-fixed at 80 mm Hg with 10% buffered formalin. The balloon-injured vessel segments, identified by 10–0 nylon sutures that had been placed proximally and distally in the periadventitial tissue, were excised. Multiple cross sections were obtained from each specimen of the proximal, mid, and distal vessel segments and placed in fresh 10% buffered formalin.

Data Analyses

Microscopy. The morphologic analyses of the arteries consisted of both a descriptive histologic and quantitative morphometric evaluations. Five-μm-thick formalin-fixed cross sections from three different segments of the carotid artery (proximal, mid, distal) were embedded in paraffin and stained with hematoxylin and eosin. The areas of the intima and the media, as well as the diameter of the arteries harvested at 9 and 21

days were measured using a digitizing measurement system (Sigma Scan, Jandel Scientific, San Rafael, CA) coupled to a camera lucida (Labophot, Nikon, Japan). Intimal area, medial area, and vessel diameter as delineated by the internal elastic lamina were measured and calculated as previously described [7].

Immunohistochemistry. To identify proliferating smooth muscle cells in the neointima, formalin-fixed specimens were incubated with the monoclonal antibody HHF-35 (Biogenics, San Ramon, CA) against smooth muscle specific α-actin, or PCNA (Proliferating Cell Nuclear Antigen, PC 10, Dako, Santa Barbara, CA) as previously described [16]. Briefly, the sections were exposed to rat adsorbed, biotinylated horse antimouse immunoglobulin for 30 minutes and subsequently incubated with horseradish peroxidase (both Vector ABC Standard Elite Kit, Vector Laboratories, Burlingame, CA). Diaminobenzidine tetrahydrochloride (DAB Substrate Kit, Vector Laboratories, Burlingame, CA) was used as chromogen and nuclear fast red as counterstain. Untreated arteries and ileum served as controls. Proliferating smooth muscle cells were identified by comparing both immunohistochemical staining. The number of PCNA-positive smooth muscle cells in the midsegments were counted in the intima in 4 high power fields (hpf) and averaged.

BPD Uptake and Localization Studies

Additional animals were used to determine serum concentration, total tissue content, and the drug distribution of BPD in the arterial wall. These measurements were performed after local delivery (LD; n = 4) and systemic delivery (SD; n = 5). In a pilot study, 2 mg/kg BPD i.v. administered 1 hour prior to excision, resulted in tissue concentrations comparable to those obtained 15 minutes after local delivery (data not shown). For the present study, a solution of 2 mg/ml BPD was injected through a 0.45 μm cellulose-acetate filter (Gelman Sciences, Ann Arbor, MI) into the femoral vein immediately after balloon injury of the common carotid artery.

Quantification of BPD Serum Concentration. An arterial line was inserted into the abdominal aorta via cannulation of the superficial femoral artery, and blood samples were drawn 2, 5, 10, and 15 minutes after local delivery, or 5, 10, 15, 30, and 60 minutes following intravenous injection of BPD. The serum was separated from the cellular constituents by centrifugation of the blood at 1,500 rpm for 10 minutes (Eppendorf Centrifuge 5415, Eppendorf Gerätebau GmbH, Hamburg, Germany) and stored at 4°C.

A spectrofluorimetric method was used to determine the serum BPD concentration. The excitation wavelength of the spectrofluorimeter (SPEX 1680, SPEX Industries, Edison, NJ) was set to 450 nm, and the samples were scanned from 550 to 800 nm, at 2-nm increments with a 0.5 second integration time. For each animal, the fluorescence signal of a serum sample drawn right before delivery of BPD was considered as background and subtracted from each subsequent reading. The area under the curve was calculated using a computer software (SPEX dM 3000, SPEX). Final photosensitizer concentrations were determined from a standard curve of a known BPD concentration in 20% fetal calf serum.

Extraction of BPD from arterial tissue. The arteries were excised immediately after drainage of the last blood samples. For BPD tissue extractions, a sample of each specimen was weighed, placed in DMSO, and homogenized. After overnight incubation in DMSO and centrifugation, the supernatants were analyzed with the spectrofluorimeter. A standard curve was obtained using a solution of 2 mg/ml BPD in DMSO.

Fluorescence microscopy. To compare the distribution of BPD in the arterial wall after local and systemic drug delivery, fluorescence microscopy was performed. Briefly, representative cross sections from the proximal, mid, and distal portion of each arterial specimen were rinsed with saline, embedded in Tissue tek O.C.T. compound® (Miles, Elkhart, IN), and stored at −70°C. Five-μm-thick cross sections were covered with PBS for index matching and examined with an epi-illumination fluorescence microscope (Axiophot, Zeiss, Oberkochen, Germany). The microscope was equipped with a SIT video camera (DAGE-MTI SIT 66, DAGE-MTI, Michigan City, IN), and an image averager (Image-II, Nippon Avionics, Tokyo, Japan), which were connected to a Macintosh II computer (Apple Computer, Cupertino, CA). Fluorescent images were obtained using excitation wavelengths between 300 and 540 nm and an emission long pass filter at 694 nm. Normal, nonphotosensitizer impregnated arteries demonstrated no fluorescence at these parameters.

Statistical Analysis

All data is expressed as mean ± standard error of the mean and compared using a one-way

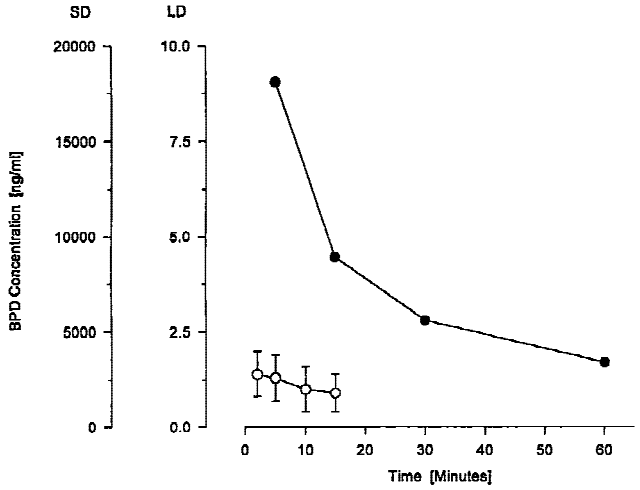

Fig. 1. Graph of benzoporphyrin-derivative serum concentration after systemic delivery (closed circles) **(SD)** and local delivery (open circles) **(LD),** plotted against the time. Values are expressed as mean ± standard error of the mean. All local delivery values (n = 4/time point) are significantly ($P < 0.001$, t-test for independent variables) lower than systemic delivery values (n = 5/time point).

analysis of variance. Differences between pairs of means were analyzed with Tukey's honestly significant difference (HSD) test (Statistica, Version 5.0, Statsoft, Tulsa, OK) and considered significant at the $P < 0.05$ level. BPD uptake data of LD vs. SD were compared with a t-test for independent variables.

RESULTS

At harvest, all animals appeared healthy without evidence of weight loss or wound infections. Animals subjected to BPD presented with no signs of systemic phototoxicity. No thrombosis was observed in any of the groups.

BPD Serum Concentration

Local delivery of BPD resulted in significantly lower serum concentrations as compared with systemic delivery ($P < 0.0001$). Two minutes after local delivery, 1.4 ± 0.6 ng/ml were extracted from the serum. At 15 minutes, this concentration dropped by ~40% to an average of 0.9 ± 0.5 ng/ml (Fig. 1).

Immediately (5 min) following systemic delivery of BPD, the serum drug concentration was 18,100 ± 1,500 ng/ml and decreased by 50% in the first 10 minutes to 8,900 ± 1,100 ng/ml (Fig.1). However, even after 60 minutes, 3,700 ± 700 ng/ml could be measured in the serum.

BPD Tissue Concentrations

Fifteen minutes after local delivery, 2.5 ± 0.7 ng/mg BPD were extracted from the vessel wall. However, no detectable quantities of BPD were retrieved from the contralateral, untreated common carotid artery. In the systemic delivery group, the carotid arteries were excised 60 minutes after intravenous injection. At that time, 1.4 ± 0.5 ng/mg BPD were extracted from both, the balloon-injured and contralateral, noninjured carotid artery.

Fluorescence Microscopy

There was no detectable fluorescence in arteries of animals that had not been subjected to BPD. Figure 2 summarizes the findings in the carotid artery after local or systemic photosensitizer delivery: 15 minutes after local delivery of BPD to balloon-injured arteries, fluorescence was detected in the entire thickness of the arterial wall (Fig. 2). The highest intensity was seen in the medial layers closest to the lumen. No fluorescence was detected from the elastic laminae, whereas a relatively weak signal was obtained from the adventitial tissue.

One hour after intravenous injection of 2 mg/kg BPD, a less bright signal was detected in the balloon-injured artery (Fig. 2). The fluorescence in the media was increased compared with the adventitia. Again, no fluorescence was seen in the internal elastic lamina. However, there were some few bright areas in the adventitia, identified as vasa vasorum. In general, the distribution patterns of locally delivered BPD and systemically delivered BPD in balloon-injured arteries were similar. From the contralateral, untreated artery (Fig. 2), only the endothelium retained significant fluorescent intensity after systemic drug delivery, whereas the media and adventitia presented with very little fluorescence.

Light Microscopy and Morphometric Analyses

Histology of arterial specimens at 9 days demonstrated slight to moderate formation of IH in BI and PR. PDT-treated arteries presented with a denuded luminal surface without evidence of gross platelet adhesion, microthrombi, inflammation, or intimal thickening (Fig. 3). Morphometric analysis revealed that balloon-injured arteries expressed the largest intimal areas with 0.19 ± 0.02 mm^2 vs. PR (0.01 ± 0.004 mm^2; $P < 0.0002$) and PDT (0 ± 0 mm^2; $P < 0.0002$) (Fig. 4). The media of PDT arteries was devoid of smooth

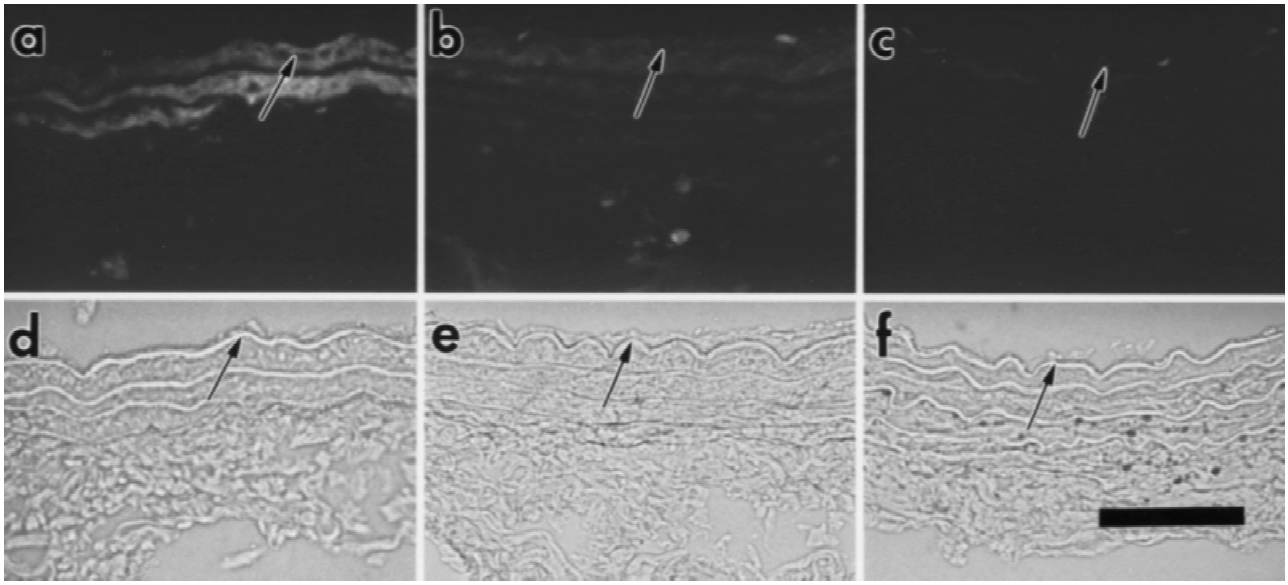

Fig. 2. Composite photomicrograph of benzoporphyrin-derivative (BPD) fluorescence in carotid arteries. The upper panels represent fluorescence images, the lower panels show light micrographs of the same section. Panels **(a) + (d):** 15 minutes after balloon injury + local delivery of BPD to the left common carotid artery. Note bright staining of the medial layers between the elastic laminae that did not take up BPD. Almost no staining of the adventitia. Panels **(b) + (e)**: 60 minutes after balloon injury of the left common carotid artery and intravenous injection of BPD. Note staining of the media with relatively brighter fluorescence of the luminal layers. BPD fluorescence was also detected in the adventitia, predominantly in vasa vasorum. Panels **(c) + (f):** right common carotid artery 60 minutes after balloon-injury and intravenous injection of BPD to the contralateral left common carotid artery. Note only the intact endothelium took up BPD. Media and adventitia were unstained. Arrows mark the internal elastic lamina.

muscle cells with the spaces between the laminae slightly diminished and filled with cellular debris. Examination of histologic cross sections of PR and BI revealed an abundance of SMC and a small number of leukocytes in the medial layers (Fig. 3).

At 21 days, intimal thickness was noted to be 0.12 ± 0.06 mm^2 in BI, 0.10 ± 0.004 mm^2 in PR and significantly less (0.01 ± 0.001 mm^2) in PDT (Fig. 4). The areas of IH in PDT-treated arteries were associated particularly with the distal or proximal ends of the treated segment. The medial areas in PR and PDT were slightly diminished compared to BI (Table 1). However, the diameter of PDT-treated arteries was slightly increased compared to BI ($P < 0.01$) (Table 1).

Over the time period studied, control arteries without any instrumentation did not show any indication of spontaneous IH or significant variation from animal to animal.

Immunohistochemistry

At 9 days, no neointima formation and no proliferative activity on the luminal surface was detected in balloon-injured arteries after local BPD-delivery and PDT. In comparison to PDT, the number of PCNA-positive smooth muscle cells was significantly higher in BI (20 ± 3 cells/hpf; $P < 0.001$ vs. PDT) and PR (25 ± 7 cells/hpf; $P < 0.001$ vs. PDT; Fig. 5). No statistically significant differences in cell proliferation could be demonstrated between BI and PR at 9 days. At 21 days, the occurrence of PCNA-positive cells was diminished in BI (10 ± 2 cells/hpf) and PR (8 ± 2 cells/hpf) without statistically significant difference. There was also no significant difference between these two groups and PDT that demonstrated an increased number of proliferating cells after 21 days as compared with 9 days (Fig. 5).

DISCUSSION

A major failure for successful treatment of IH in vivo has been associated with the inability to provide adequate concentrations of pharmacologic or other biologic compounds to vascular lesions through systemic drug delivery [17]. As a result, the concept of intravascular, site-specific delivery has evolved from concerns that serious side effects might occur when the necessary quantities of these compounds are systemically administered [18].

This study verified that local delivery of the

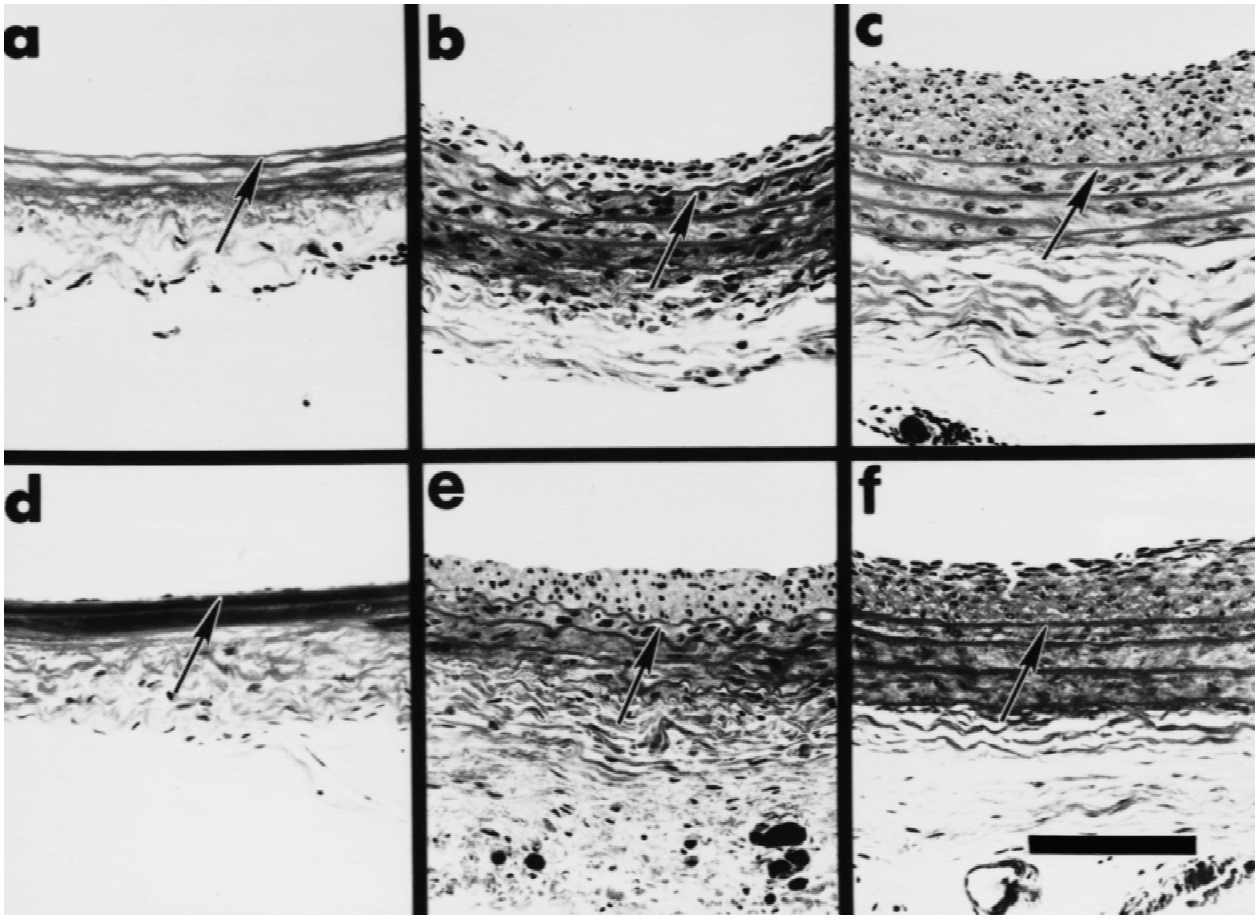

Fig. 3. Composite photomicrograph of common carotid arteries at 9 days (upper panels) and 21 days (lower panels) after PDT (panels **(a)** and **(d)**), saline pressurization (PR; panels **(b)** and **(e)**), and balloon-injury only (BI; **(c)** and **(f)**). Hematoxylin-eosin staining. Arrow depicts internal elastic lamina. Bar represents 100 μm. Note: no intimal hyperplasia or medial repopulation after local delivery and photodynamic therapy.

photosensitizer BPD can be effectively used for PDT and inhibit the development of experimental IH. PDT has been repeatedly demonstrated to be effective in limiting the formation of IH lesions in animal models after intravenous photosensitizer administration and focal light-directed irradiation [6,7,19–21]. Although photosensitizers have a proclivity to accumulate in IH tissue and atherosclerotic plaques after systemic delivery [10,12,21], there is also accumulation of the photosensitizer in other tissues, such as normal artery or skin. The indiscriminate activation by ambient light or scattered light from irradiation can result in unintentional and undesirable tissue damage to skin and perivascular injury. The best-studied model of neointimal formation is the response of the rat carotid artery to balloon angioplasty [22]. The simplicity of the rat model has facilitated kinetic analyses of the smooth muscle cell responses to injury and to the identification of molecules playing a role in the pathogenesis of IH [1,3,22]. Numerous vascular PDT studies have also applied this model, and a significant body of experience was acquired with regard to PDT dosimetry, histology, and healing responses [10,20,21,23]. However, local drug delivery to the rat artery has thus far not been attempted, because the small size of these vessels did not support the use of specialized delivery catheters such as double-balloon-, porous-, microporous-, channel-, iontophoresis, or hydrogel balloon catheters [11,17]. Therefore, in the present study, the basic principle of local delivery was employed in the rat model by direct pressurization of a vessel segment to deliver the photosensitizer. As with the double-balloon catheter, a sealed compartment was created in the carotid artery from which blood was subsequently evacuated, and BPD introduced with hyperbaric pressure.

Intraluminal pressure, duration of pressur-

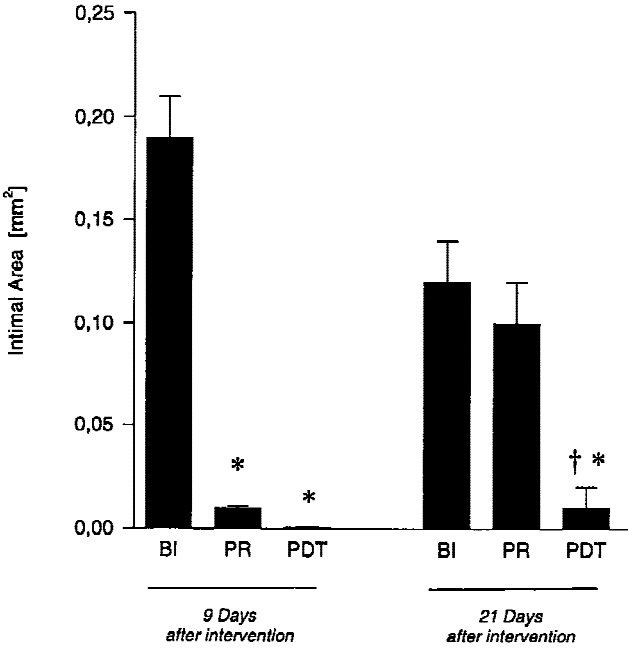

Fig. 4. Intimal areas of balloon-injury only (BI), saline-pressurization (PR), and PDT-treated arteries at 9 and 21 days after the intervention. Bars represent mean ± standard error of the mean. (*) signifies a statistically significant difference (ANOVA; $P < 0.0002$) vs. BI, (‡) signifies a $P < 0.0004$ vs. BI. (†) signifies difference (ANOVA; $P < 0.003$) compared to PR.

ization, and particle size are critical factors for the penetration depth of locally delivered substances in the arterial wall [24]. Thirty minutes after continuous hyperbaric infusion (400 mm Hg) of india ink particles with a size range of 120–500 nm, or latex spheres with diameters of ~100 nm, particles were located predominantly in the intima and in the in the vasa vasorum of the adventitia [24]. In muscular-type arteries, a pressure of 500 mm Hg applied for 45 seconds resulted in complete penetration of the subendothelium *and* the media, but was not sufficient to create homogenous penetration of the entire vascular wall with 2–6 nm sized horseradish peroxidase particles [25]. Irrespective of prior balloon-injury, the particle distribution pattern appears to be primarily attributed to anatomic barriers in the arterial wall that impose significant constraints for the penetration of larger particles through the media [24]. These anatomic barriers most likely consist of the internal elastic lamina and other fibroelastic structures [26]. The present study in elastic-type arteries after balloon-injury shows that pressurization with BPD-liposomes (particle size: 100–200 nm) at a constant pressure of 400 mm Hg results in complete penetration of the media and partial penetration of the adventitia (Fig. 2). Whereas the photosensitizer did not bind to the elastic laminae, the smooth muscle cells inbetween these laminae stained brightly with BPD. On the basis of earlier works, one would not expect particles of this size range to penetrate freely through the wall of elastic arteries. Yet, even without iatrogenic pressurization of the arterial wall, fluorescence microscopy visualized identical particle distribution patterns in the media and adventitia of balloon-injured arteries after *systemic delivery* of BPD (Fig. 2). The reason for this finding is not clear. Yet, it can be theorized that disintegration of the liposomes, or possible dissociation of BPD molecules from the liposomes might have occurred in the course of site-specific delivery and at that point permitted the smaller particles to penetrate the elastic laminae. It is also conceivable that significant BPD-penetration of the vascular wall occurred via vasa vasorum channels, which were visualized by fluorescence microscopy (Fig. 2).

Since no substantial concentration of BPD was detected in the serum following site-specific delivery, it can be reasoned that no other tissue than the targeted artery could have possibly taken up the photosensitizer. This strongly suggests that local delivery of BPD is not associated with any other effects than the cytotoxicity to the targeted arterial wall and in essence proves the rationale of this therapeutic concept. However, high serum concentrations of BPD were present after systemic delivery. One hour after intravenous injection, liposomal BPD accumulated in the endothelial cells, but not in the subendothelium, the media, or the adventitia of intact carotid arteries. This result accords with the known inability of liposomes [27] and even nonliposomal photosensitizers [10] to penetrate intact endothelium of the macrovasculature and emphasizes the "barrier function" of endothelial cells.

Another aspect of site-specific drug delivery and PDT encompasses the critical issue of combined balloon-injury, pressure- and PDT-related injury to the vascular wall, which may precipitate structural destabilization of the artery with aneurysm formation. Light microscopy of saline-pressurized arteries (PR) at 21 days indicated the presence of additional injury to the media with eradication of smooth muscle cells (Fig. 3) and a slight but statistically significant decrease of medial thickness vs. BI (Table 1). These findings are consistent with other studies using perfusion pressures of 400 mm Hg [24,25]. Pressurization of

TABLE 1. Morphometric Analyses

	9 days			21 days		
	BI[a]	PR[b]	PDT[c,d]	BI	PR	PDT[c,d]
Medial area (mm^2)	0.12 ± 0.01	0.12 ± 0.01	0.11 ± 0.005	0.13 ± 0.004	0.10 ± 0.01*	0.10 ± 0.005**
Diameter (mm)	0.82 ± 0.02	0.79 ± 0.01	0.78 ± 0.01	0.79 ± 0.02	0.82 ± 0.04	0.9 ± 0.02***

[a]Balloon-injury only.
[b]Balloon-injury + saline pressurization.
[c]Balloon-Injury + BPD-pressurization + photodynamic therapy.
[d]n-number of measurements in this group = 12.
*P < 0.03 vs. BI at the same time point; **P < 0.05 vs. BI at the same time point; ***P < 0.01 vs. BI at the same time point. All data are expressed as mean ± SEM; n-number of measurements = 9, if not otherwise stated.

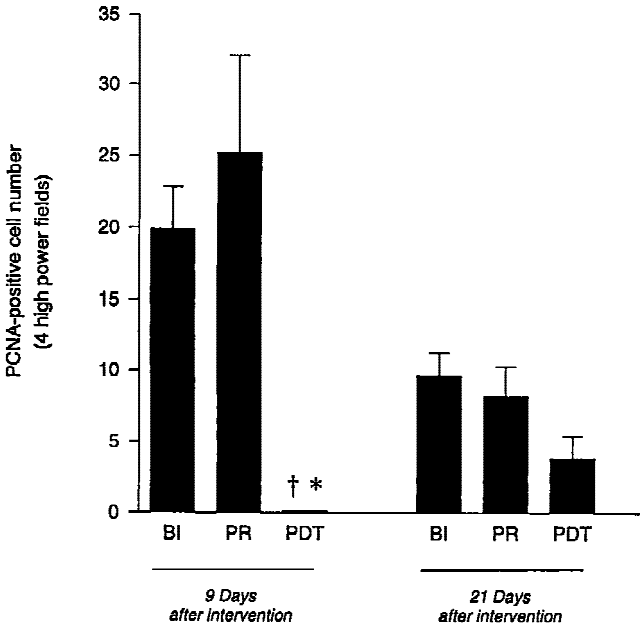

Fig. 5. Average number of PCNA positive cells per four high power fields of balloon-injury only (BI), saline-pressurization (PR), and PDT-treated arteries at 9 and 21 days after the intervention. Bar and error bar represent mean ± standard error of the mean. (*) signifies a statistically significant difference (ANOVA; P < 0.001) vs. BI, and (†) signifies difference (ANOVA; P < 0.001) compared to PR.

sheep carotid and femoral arteries with horseradish peroxidase revealed severe injuries to the vessel wall with frequent disruptions of the internal elastic lamina and accompanying microdissections in the media [24]. These studies also suggested that infusion pressures of 150 mm Hg were both nontraumatic [24,25] and sufficient for the uptake of deoxyribose nucleic acid (DNA) plasmids into the arterial wall for gene-therapy. In a pilot study, we attempted local delivery of BPD with perfusion pressures of 100 and 200 mm Hg, respectively (data not shown). Although, the use of lower perfusion pressures was less traumatic to the vascular wall, PDT could not be prevented IH at 2 weeks.

When the pressure injury to the artery was followed by PDT of the vascular wall, a small diameter increase was noted at 21 days (Table 1). Previous studies from this laboratory have shown that possible sequelae of PDT-associated eradication of medial SMC are loss of vasomotor tone, reduction of circumferential compliance, and minimal, although significant, diameter increase [28]. This diameter increase, which never exceeded 15% vs. control, has thus far not demonstrated a tendency of continuous growth and aneurysm formation for up to 16 weeks [20]. Others have systematically investigated the effects of PDT on the mechanical integrity of arteries and could not find any differences between PDT- and control vessels [29]. Nonetheless, it is not known if PDT, in addition to local pressurization, results in continued vessel dilation and aneurysm formation on a long-term basis.

Following pressure-induced injury of blood vessels, proteins are released from dead or injured cells that include potent mitogens capable of initiating a secondary wave of cell proliferation [17]. Immunohistochemical studies of arteries revealed that shortly after balloon-injury, a wide array of growth factors and cytokines such as bFGF [30,31] and PDGF [32] are released in the vascular wall. The amount of growth factor release correlates with the severity of the injury [33]. The results of the present study verified an increased number of proliferating smooth muscle cells and substantial IH in balloon-injured arteries (BI) after 9 days. In contrast, a significantly increased number of proliferating smooth muscle cells in PR was *not* accompanied by an enlarged intimal area (Figs. 4 and 5). Only 2 weeks later, however, the intimal area of PR arteries was enlarged by almost 10-fold with no notable differences between BI and PR. This finding agrees with previous experimental observations in rabbit iliac arteries, which suggest that the use of a porous balloon catheter does not produce more vas-

cular injury than conventional angioplasty alone. In these studies, light microscopy revealed endothelial denudation and nonspecific medial changes, scanning electron microscopy showed crater formation with medial penetration corresponding to jet effects of the balloon pores [25]. In the present study, IH development in PR was probably delayed due to pressure-induced cell death in the media, but subsequently accelerated because of increased smooth muscle cell proliferation after vascular injury, as implied by the high number of PCNA-positive cells. In PDT-treated arteries, IH development was primarily limited to the proximal and distal perimeter of the treatment area and diminished toward the center. This particular distribution pattern of IH lesions had been linked to mechanical, clamp-induced injuries with subsequent migration of smooth muscle cells from the edges to the center [20].

Besides balloon-injury and local BPD pressurization, PDT represents an additional traumatic injury to the arterial wall. This could be associated with the release of vast amounts of growth factors and the prevalence of a large number of proliferating cells. Since no such observations and no inflammatory response were noted, it is conceivable that PDT not only eliminated the entire population of IH-inducing smooth muscle cells, but also modified the extracellular matrix in the vascular wall, which is known to contain or bind biologically active proteins. Recent in vitro studies from this laboratory suggest that PDT alters extracellular matrix, probably by dose-dependent growth factor inactivation and thus inhibits smooth muscle cell attachment, proliferation, and migration [34,35]. These in vitro findings correspond with previous in vivo studies [7,20,21,23] and observations of the present study, which reveal an acellular media even 21 days after PDT, whereas PR arteries, at the same time, display complete repopulation of the media with smooth muscle cells.

As in many experimental studies, the major limitation of this investigation is related to the animal model and the delivery mode used. Although the balloon-injury model produces considerable smooth muscle cell proliferation and IH, it is well recognized that this response may not represent the prototype of an obstructive lesion in humans. Nevertheless, PDT utilizing the local drug delivery concept can be performed safely and appears promising as a preventive strategy against IH.

ACKNOWLEDGMENTS

The authors thank Norman Michaud, Margaret Sherwood, Bart Johnson, and Kathy Roberts for help with the processing of the histological specimens and the preparation of the photographs. We gratefully acknowledge Drs. R. Rox Anderson, Nikoforos Kollias, Gloria Lin, and Phillipe Margaron of QLT for many helpful discussions, and Dr. John Parrish for his continuing support. The BPD-MA Verteporfin® was a generous gift by Quadra Logic Technologies, Vancouver, Canada, and the Fogarty embolectomy catheters were kindly provided by Baxter Healthcare, Irvine,CA.

REFERENCES

1. Davies MG. Pathobiology of intimal hyperplasia. Br J Surg 1994;81:1254–1269.
2. Kumpe DA, Becker GJB. Percutaneous transluminal angioplasty and other endovascular technologies. In: Rutherford RB, ed. "Vascular Surgery," 4th ed. Philadelphia, PA: W.B. Saunders Company, 1995:352–94. vol 1.
3. Clowes AW, Reidy MA. Prevention of stenosis after vascular reconstruction: Pharmacologic control of intimal hyperplasia-A review. J Vasc Surg 1991;13:885–91.
4. Leclerc G, Gal D, Takeshita S, Nikol S, Weir L, Isner JM. Percutaneous arterial gene transfer in a rabbit model. Efficiency in normal and balloon-dilated atherosclerotic arteries. J Clin Invest 1992;90:936–44.
5. Lee SW, Trapnell BC, Rade JJ, Virmani R, Dichek DA. In vivo adenoviral vector-mediated gene transfer into balloon-injured rat carotid arteries. Circ Res 1993;73:797–807.
6. Eton D, Colburn MD, Shim V, et al. Inhibition of intimal hyperplasia by photodynamic therapy using photofrin. J Surg Res 1992;53:558–62.
7. Ortu P, LaMuraglia GM, Roberts WG, Flotte TJ, Hasan T. Photodynamic therapy of arteries. A novel approach for treatment of intimal hyperplasia. Circulation 1992; 85:1189–96.
8. Dubbelman TMAR, Prinsze C, Penning LC, van Steveninck J. Photodynamic Therapy: Membrane and Enzyme Photobiology. In: Henderson BW, Dougherty TJ, eds. Photodynamic therapy. Basic principles and clinical applications. New York: Marcel Dekker, Inc., 1992:37–46.
9. Hilf R. Cellular targets of photodynamic therapy as a guide to mechanisms. In: Henderson BW, Dougherty TJ, eds. Photodynamic therapy. Basic principles and clinical applications. New York: Marcel Dekker Inc., 1992:47–54.
10. LaMuraglia GM, Ortu P, Flotte TJ, et al. Chloroaluminum sulfonated phthalocyanine partitioning in normal and intimal hyperplastic artery in the rat. Implications for photodynamic therapy. Am J Pathol 1993;142:1898–905.
11. Lincoff AM, Topol EJ, Ellis SG. Local drug delivery for the prevention of restenosis. Fact, fancy, and future. Circulation 1994;90:2070–83.
12. Hsiang YN, Crespo MT, Richter AM, Jain AK, Fragoso M,

Levy JG. In vitro and vivo uptake of benzoporphyrin derivative into human and miniswine atherosclerotic plaque. Photochem Photobiol 1993;57:670–4.
13. Aveline B, Hasan T, Redmond RW. Photophysical and photosensitizing properties of benzoporphyrin derivative monoacid ring A (BPD-MA). Photochem Photobiol 1994; 59:328–35.
14. Pass HI. Photodynamic therapy in oncology: mechanisms and clinical use. J Natl Cancer Inst 1993;85:443–56.
15. Schmidt-Erfurth U, Hasan T, Schomaker K, Flotte T, Birngruber R. In vivo uptake of liposomal benzoporphyrin derivative and photothrombosis in corneal neovascularization. Lasers Surg Med 1995;17:178–88.
16. LaMuraglia GM, Adili F, Schmitz-Rixen T, Michaud NA, Flotte TJ. Photodynamic therapy inhibits experimental allograft rejection. A novel approach for the development of vascular bioprostheses. Circulation 1995;92:1919–26.
17. Riessen R, Isner JM. Prospects for site-specific delivery of pharmacologic and molecular therapies. J Am Coll Cardiol 1994;23:1234–44.
18. March KL, Wilensky RL, Hathaway DR. Novel drug and device combinations for targeted prevention of restenosis. Cardio Intervention 1992;2:11–26.
19. Hsiang YN, Houston G, Crespo MT, et al. Preventing intimal hyperplasia with photodynamic therapy using an intravascular probe. Ann Vasc Surg 1995;9:80–6.
20. LaMuraglia GM, ChandraSekar NR, Flotte TJ, Abbott WM, Michaud N, Hasan T. Photodynamic therapy inhibition of experimental intimal hyperplasia: Acute and chronic effects. J Vasc Surg 1994;19:321–31.
21. Nyamekye I, Anglin S, McEwan J, Alexander M, Bown S, Bishop C. Photodynamic therapy of normal and balloon-injured rat carotid arteries using 5-amino-levulinic acid. Circulation 1995;91:417–25.
22. Schwartz SM, deBlois D, O'Brien ERM. The intima. Soil for atherosclerosis and restenosis. Circ Res 1995;77:445–65.
23. Grant WE, Speight PM, MacRobert AJ, Hopper C, Brown SG. Photodynamic therapy of normal rat arteries after photosensitisation using disulphonated aluminium phthalocyanine and 5-aminolaevulinic acid. Br J Cancer 1994;70:72–78
24. Rome JJ, Shazani V, Flugelman MY, et al. Anatomic barriers influence the distribution of in vivo gene transfer into the arterial wall. Modeling with microscopic tracer particles and verification with a recombinant adenoviral vector. Arterioscler Thromb 1994;14:148–61.
25. Goldman B, Blanke H, Wolinsky H. Influence of pressure on permeability of normal and diseased muscular arteries to horseradish peroxidase. A new catheter approach. Atherosclerosis 1987;65:215–25.
26. Wolinsky H. Local delivery: Let's keep our eyes on the wall. J Am Coll Cardiol 1994;24:825–7.
27. Poiani GJ, Wilson FJ, Fox JD, et al. Liposome-entrapped antifibrotic agent prevents collagen accumulation in hypertensive pulmonary arteries of rats. Circ Res 1992;70: 912–22.
28. L'Italien GJ, ChandraSekar NR, LaMuraglia GM, et al. Biaxial elastic properties of rat arteries in vivo: influence of vascular wall cells and anisotropy. Am J Physiol 1994; 267:11574–9.
29. Grant WE, Buonaccorsi G, Speight PM, MacRobert AJ, Hopper C, Bown SG. The effect of photodynamic therapy on the mechanical integrity of normal rabbit carotid arteries. Laryngoscope 1995;105:867–71.
30. Olson EN, Chao S, Lindner V, Reidy MA. Intimal smooth muscle cell proliferation after balloon catheter injury. The role of basic fibroblast growth factor. Am J Pathol 1992;140:1017–23.
31. Villaschi S, Nicosia RF. Angiogenic role of endogenous basic fibroblast growth factor released by rat aorta after injury. Am J Pathol 1993;143:181–90.
32. Majesky M, Reidy M, Bowen-Pope D, Hart C, Wilcox J, Schwartz S. PDGF ligand and receptor gene expression during repair of arterial injury. J Cell Biol 1990;111: 2149–58.
33. Jackson CL, Reidy MA. Basic fibroblast growth factor: Its role in the control of smooth muscle cell migration. Am J Pathol 1993;143:1024–31.
34. Adili F, Statius van Eps RG, Karp SJ, Watkins MT, LaMuraglia GM. Differential modulation of vascular endothelial and smooth muscle cell function by photodynamic therapy of extracellular matrix: novel insights into radical-mediated prevention of intimal hyperplasia. J Vasc Surg 1996;23:698–705.
35. Statius van Eps RG, Adili F, LaMuraglia GM. Photodynamic therapy inactivates cell-associated basic fibroblast growth factor: a silent way of vascular smooth muscle cell eradication. Cardiovascular Research 1997; 35:334–340.